



## Abstract

In the frame of the European project, entitled MULTI-ASSESS, specimens of structural metals, glass, stone and concrete materials were exposed to air pollution at a station, which was installed for this purpose on a building, located in the centre of Athens. The main purpose of this project was to determine the corrosion and soiling effects of air pollution on materials. A set of the specimens was exposed in a position that was sheltered from rain and partly from wind, and another set was exposed in unsheltered positions on the roof of the above said building. In addition, other specimens were exposed at different heights on the same building, in order to investigate for the first time the corrosion and soiling effects on various materials as a function of height. For the determination of these effects, chemical analysis of the specimens was performed and basic parameters as the weight change, the layer thickness and the optical properties were calculated. Finally, the results obtained are discussed and their plausible interpretation is attempted.

## 1 Introduction

It is well known that air pollution influences human health and ecosystems affecting also various materials via corrosion and soiling mechanisms (Varotsos et al., 1995; Kondratyev and Varotsos, 1996; Katsambas et al., 1997; Alexandris et al., 1999; Feretis et al., 2002; Ferm et al., 2005, 2006; Methven et al., 2006; Chattopadhyay and Chattopadhyay, 2008; Tzanis and Varotsos, 2008; Varotsos et al., 2009). The atmospheric corrosion of materials is related to the acidification of the air, induced by gases such as  $\text{SO}_2$  and  $\text{HNO}_3$ . Actions against this problem have had satisfactory results, succeeding in reducing  $\text{SO}_2$  concentration. Increased usage of cars has transformed the pollution situation by increasing the concentrations of other corrosive pollutants, like nitrogen compounds, particulate matter and ozone (Monks et al., 2000; Cape et al., 2004; Friess et al., 2006; Heard et al., 2006; Ondov et al., 2006; Ebel et al., 2007).

## Corrosion and soiling effects by air pollution

C. Tzanis et al.

Title Page

Abstract

Introduction

Conclusions

References

Tables

Figures



Back

Close

Full Screen / Esc

Printer-friendly Version

Interactive Discussion



The European Commission, under the Fifth Framework Programme Key Action City of Tomorrow and Cultural Heritage, funded a research project entitled MULTI-ASSESS (Model for multi pollutant impact and assessment of threshold levels for cultural heritage) (Kucera et al., 2005) with the objective of studying this new situation and especially the deterioration of materials due to air pollution and climate by developing new dose response functions and soiling models (Tzanis et al., 2009). 34 European sites from all over Europe and one from Canada participated in the project.

## 2 Experimental

The MULTI-ASSESS project was divided into seven work packages (WPs). The University of Athens has participated in WP1, WP2 and WP4. The main experimental observations were obtained in the frame of WP4, which took place during 2003-2004, and are presented here. More specifically in this work package, specimens of structural metals, glass, natural and artificial stone materials were exposed to different environmental conditions. Some of these materials were selected because they have been used in the construction of monuments, while the rest of them are often used in the construction of modern buildings. For the purpose of this project, a station was installed on the building of the Ministry of Health and Social Solidarity of Greece (37°59'16" N, 23°43'39" E) in Aristotelous Street (shown in the top panel of Fig. 1). This building is located in central Athens next to the "ring road", at a crossroads. One facade of the building is facing south, whilst the other faces to the east.

Some of the specimens were exposed on the roof, while the rest of them were exposed at specific height levels on the east facade of the building. Due to the needs of the experiment two kinds of racks were installed at this building. A wooden rack (the main rack) was installed on the roof, facing south, while a group of three aluminium racks were installed on the ground floor, the 1st, 2nd, 4th, 5th and 7th floor (height levels of 3 m, 6 m, 9 m, 15 m, 18 m and 21 m from the ground, respectively). The wooden rack consisted of an inclined plane, for the specimens' display under

### Corrosion and soiling effects by air pollution

C. Tzanis et al.

Title Page

Abstract

Introduction

Conclusions

References

Tables

Figures

◀

▶

◀

▶

Back

Close

Full Screen / Esc

Printer-friendly Version

Interactive Discussion



unsheltered conditions, and an aluminium box with open bottom, for the exposure of specimens under sheltered conditions (see the bottom panel of Fig. 1). The display of the aluminium racks was under sheltered conditions and they were distributed on the east facade of the building (see top and middle panel of Fig. 1).

5 The exposed structural metal samples included zinc (99.99%), copper (Cu 99%, P 0.015 to 0.04%), unalloyed carbon steel (C<0.2%, P<0.07%, S<0.05%, Cu<0.07%) and bronze (Cu 81%, Sn 5.8%, Pb 6.7%, Zn 4.5%, Ni 1.6% and trace elements). Three samples of each material were exposed at an unsheltered situation on the inclined plane of the main rack for one year. All the samples had the same dimensions (100×150×(1–2) mm<sup>3</sup>).  
10 Two samples of zinc, copper and steel were exposed at each height level, mounted on the aluminium racks for one year. All the samples had the same dimensions, but different from the samples exposed on the main rack (100×50×(1–2) mm<sup>3</sup>).

Two different types of glass were exposed, medieval glass (SiO<sub>2</sub> 48%, K<sub>2</sub>O 25.5%, CaO 15%, MgO 3%, Al<sub>2</sub>O<sub>3</sub> 1.5%, P<sub>2</sub>O<sub>5</sub> 4%, Na<sub>2</sub>O 3%, in mass percentage) and modern glass (SiO<sub>2</sub> 71.7%, Na<sub>2</sub>O 13.1%, CaO 9.6%, MgO 4.1%, K<sub>2</sub>O 0.3%, Al<sub>2</sub>O<sub>3</sub> 0.7%, Fe<sub>2</sub>O<sub>3</sub> 0.1%, in mass percentage). Six samples of medieval glass (10×10×2 mm<sup>3</sup>),  
15 mounted three on each of two glass-fibre reinforced plastic plates, were exposed in the aluminium box, while four samples, mounted two on each of two of the same kind of plastic plates, were exposed at the specified levels. The duration of the exposure was 6 months for half of the specimens and one year for the other half. Modern glass samples were exposed on the main rack. Eight samples, mounted on a wooden plate, were placed on the inclined plane and another group of eight samples, mounted on an aluminium plate, was placed into the aluminium box. All specimens had the same dimensions (100×100×2 mm<sup>3</sup>).  
20 Every three months a sample of each group was withdrawn. During the experiment it was decided to expose the last two specimens of each group for a longer time period.

25 The natural stone materials included Carrara marble (Italy), Baumberger sandstone (Germany), Gotland sandstone (Sweden), Saaremaa dolomite (Estonia) and three

**Corrosion and soiling effects by air pollution**

C. Tzanis et al.

Title Page

Abstract

Introduction

Conclusions

References

Tables

Figures

⏪

⏩

◀

▶

Back

Close

Full Screen / Esc

Printer-friendly Version

Interactive Discussion



types of Portland limestone (England) with smooth, medium and rough surfaces. In parenthesis the country of origin of each material is depicted. Figure 2 shows the physical properties of the natural stone materials. Reference concrete was used as artificial stone material, prepared in laboratory conditions, using Portland cement CEM I 32.5N, fine-middle aggregates, Water/Cement (W/C) ratio 0.7 and having: apparent density: 2294 kg m<sup>-3</sup>, open porosity: 16.8%, water absorption: 5.7%, saturation coefficient: 0.8.n (Tidblad et al., 2005). All the samples had the same dimensions (50×50×(8±2) mm<sup>3</sup>). Three samples of each material, medium type for Portland limestone, were exposed as sheltered and unsheltered on the main rack, mounted on special carousels. Half of the samples were withdrawn after one year of exposure, while the rest of the samples remained exposed for two years. In addition, two samples of each type of Portland and concrete were exposed at the specific height levels, mentioned above.

### 3 Results and discussion

#### 3.1 Structural metals

In order to investigate the corrosion behaviour of structural metals, weight change and mass loss were studied. Figure 3 shows the measurements obtained for the weight change of the exposed specimens at the specific height levels. It should be kept in mind that the weight change is defined as the difference between the mass of an exposed sample and its initial mass before the exposure. Obviously the weight change depends on the particular environmental conditions. In this context, under sheltered conditions, where there is no run-off (material loss into the environment; Singer et al., 2003), weight change is always positive, because of the uptake of material from the environment. Under unsheltered conditions, except of the uptake process, the run-off of dissolved metal or patina components leads to a diminution of environmental compounds and weight change can be positive or negative (Tidblad et al., 1998). According to the results obtained, the unalloyed carbon steel is the most sensitive metal, among the

## Corrosion and soiling effects by air pollution

C. Tzanis et al.

Title Page

Abstract

Introduction

Conclusions

References

Tables

Figures

◀

▶

◀

▶

Back

Close

Full Screen / Esc

Printer-friendly Version

Interactive Discussion



exposed ones, to weight change, while copper is the most durable. The highest value of weight change for the steel was noticed at the level of 18 m, while the lowest at the level of 6 m. For zinc and copper specimens values of weight change were almost constant with the height.

5 The experimental results of the mass loss, for the same specimens, are presented in Fig. 4. Keeping in mind that the mass loss is defined as mass difference between the original metal and the remaining metal after removing the corrosion layer, we reach to the conclusion that this parameter is directly correlated to the loss of metal due to run-off and compounds within the corrosion layer. The unalloyed carbon steel arises to  
10 be the most sensitive metal, among the exposed ones, to the mass loss, while copper is the most durable. For all the metals, the lowest values were noticed at the level of 6 m with an increase with the height.

The same parameters were also estimated for the specimens exposed as unsheltered on the main rack. The results for the weight change can be seen in Fig. 5. Un-  
15 alloyed carbon steel was the material with the greatest value of weight change, while bronze was the only material with negative value of this parameter. The latter result can be explained by considering the influence of run-off on the specimens exposed under unsheltered conditions, which cause diminution of environmental compounds.

Figure 6, illustrates the results for the mass loss of the same specimens as above.  
20 These results confirm that the unalloyed carbon steel is the most sensitive material to the corrosion. Copper and bronze, with almost equal values of mass loss, suffered less by atmospheric corrosion. Zinc mass loss values were almost 70% greater than the same values of copper and bronze.

25 The concentration of the water-soluble anions within the corrosion layer was analysed by IC (ion chromatography) (Horalek et al., 2005). At the first step of this analysis, specimens were rinsed in 25 ml deionised water ( $<0.1 \mu\text{S cm}^{-1}$ ) for 5 min on each side. The extracted components were filtered through a  $45 \mu\text{m}$  acetyl cellulose filter, at the next step and finally the solution was stored in polyethylene bottles before the analyses. The results for the copper specimens, exposed at the specific levels, are presented in

**Corrosion and soiling effects by air pollution**

C. Tzanis et al.

Title Page

Abstract

Introduction

Conclusions

References

Tables

Figures

◀

▶

◀

▶

Back

Close

Full Screen / Esc

Printer-friendly Version

Interactive Discussion



Fig. 7. Sulphate dominates among the water soluble anions, while nitrate concentrations are also high. Chloride concentrations are lower than nitrate. The water soluble anion with the lowest concentration detected is fluoride. Concentrations of nitrate, chloride and fluoride decrease with height against sulphate concentration, which increasing up to the level of 18 m.

The results of the IC analyses of the copper and bronze specimens exposed on the main rack (unsheltered) are presented in Fig. 8. Sulphate is the anion with the highest concentration followed by chloride, unlike the sheltered ones, where nitrate was the anion with the second higher concentration, nitrate and fluoride. These anions, except sulphate, had almost equal concentrations on both materials. The concentration of sulphate detected was 25% greater on bronze than on copper. The data for unsheltered samples should be used with caution because even a single rain occurrence can influence them.

### 3.2 Medieval glass

The most critical parameter for the specification of the weathering of medieval glass specimens is the leaching depth of the constituents and especially K and Ca ( $d(K)$ ,  $d(Ca)$ ) because these elements present the most significant deterioration. After the appropriate preparation of the samples (Melcher and Schreiner, 2004) these parameters were measured using scanning electron microscopy (SEM) in combination with energy dispersive x-ray microanalysis (EDX). Mean values of the leaching depths have been calculated for the specimens exposed for 6 and 12 months. The results obtained from the specimens exposed on the main rack (sheltered) are presented in Fig. 9. According to these results, K is the element with the highest leaching depth. The rate of increase of leaching depth for the first 6 months was  $0.16 \mu\text{m month}^{-1}$  and  $0.12 \mu\text{m month}^{-1}$  for K and Ca, respectively. For the next 6 months these rates were decreased to  $0.095 \mu\text{m month}^{-1}$  for both elements. These results indicate that the rate of increase of leaching depth for K was decreased 2.5 times more than the rate of increase of leaching depth for Ca.

## Corrosion and soiling effects by air pollution

C. Tzanis et al.

Title Page

Abstract

Introduction

Conclusions

References

Tables

Figures

◀

▶

◀

▶

Back

Close

Full Screen / Esc

Printer-friendly Version

Interactive Discussion



In Fig. 10, the results of the  $d(K)$  and  $d(Ca)$  for the specimens exposed at specific levels (sheltered) are presented. The highest values, for both elements and for the two periods, were observed at the level of 21 m, which is almost at the same height as the main rack. A second maximum was observed at the level of 15 m also for both elements and for the two periods. The main weathering products detected on the specimens via surface analyses were syngenite ( $CaSO_4 \cdot K_2SO_4 \cdot H_2O$ ) and gypsum ( $CaSO_4 \cdot 2H_2O$ ). As is seen in this figure, values of leaching depth of K are higher than the values of leaching depth of Ca. A possible explanation for this could be the greater mobility of K, compared to the mobility of Ca (Melcher and Schreiner, 2006).

In Fig. 11, the rates of leaching depth increase for all the specimens and for both elements, K and Ca, are presented. The highest values were noticed at the level of 21 m (main peak) and at the level of 15 m (secondary maximum). It is remarkable that these rates had increased with time, unlike what was observed for the rates of the specimens exposed on the main rack. The only exceptions were the rate for K, at the level of 21 m, and the rate for Ca, at the level of 18 m, which had been decreased with time. The values of  $d(d(K)6)/dt$  and  $d(d(Ca)6)/dt$  were calculated by dividing by 6 the measurements of leaching depth for the 6 months exposure. The values of  $d(d(K)12)/dt$  and  $d(d(Ca)12)/dt$  were calculated by dividing by 6 the difference of leaching depth of 6 months exposure from the leaching depth of 12 months exposure.

### 3.3 Modern glass

Modern glass is a material of great concern since it is widely used in contemporary urban architecture. As a substrate, it does not influence the particle deposition and accumulation because it is chemically inert, transparent and its surface is flat, smooth and non-porous; consequently, it is an ideal material for the investigation of soiling (Ionescu et al., 2006; Lombardo et al., 2005, 2010).

(a) First, if one studies soiling at a macroscopic scale, its time evolution gives some characteristics about this phenomenon. The total deposited mass of particles per surface unit of glass (TP/S) and haze (ratio in % between the diffuse and the direct

## Corrosion and soiling effects by air pollution

C. Tzanis et al.

Title Page

Abstract

Introduction

Conclusions

References

Tables

Figures

⏪

⏩

◀

▶

Back

Close

Full Screen / Esc

Printer-friendly Version

Interactive Discussion



transmitted light) were measured in order to characterize the soiling of the exposed glass samples (sheltered), during almost 3 years. TP/S was determined by weighing the samples before and after exposure, using a Metler AE240 Balance, the mass being divided by the surface of each sample. The haze was determined by using a UV-VIS spectrometer Lambda 650 Perkin Elmer. The results (Ionescu et al., 2006) are presented in Fig. 12 which shows experimental points and the best-fit model, which in this case is based on the Hill equation, also known as the variable slope sigmoid:  $Y(t) = B + K / (1 + (M/t)^H)$  where  $t$  represents time,  $B$  corresponds to the initial and  $B + K$  to the saturation levels of  $Y$  (thus  $K$  represents the span),  $M$  represents time when  $Y$  is halfway between  $B$  and  $B + K$ , and  $H$  is the maximum slope of the curve. Indeed, for different exposure sites in different cities in Europe, including Athens, the measurements of soiling at different periods, expressed in terms of haze or TP/S, revealed a sigmoidal shape and Hill's equation fitted the best. In addition, the time variation expressed by this curve has a plausible physical interpretation in terms of soiling rate: at the beginning, a very slow rate (the substrate for the particle deposit is glass, which is smooth), then the substrate glass+particles becomes rougher and the deposition rate increases progressively up to a maximum rate; some of the particles are removed (e.g. by the wind) and the soiling rate results from two simultaneous phenomena: deposition and removal. When deposition and removal attain equilibrium, soiling attains saturation.

The general increasing trend demonstrates a cumulative non-linear phenomenon with an asymptotic level of saturation. The same general trend was found for the other sites involved in the MULTI-ASSESS project (London, Krakow, Prague, Rome), with the particularity that the saturation level was different from site to site, probably related to the environmental level of pollution. Indeed, a dose-response function has been established to relate soiling, via the haze, to the most influent parameters, which were found to be  $PM_{10}$ ,  $SO_2$  and  $NO_2$ : 43%, 39% and 19% contributions to explain haze variance (Lombardo et al., 2010). It is interesting now to test to what extent the influence of the environmental pollutants, revealed by the statistical analysis, can be confirmed by a chemical analysis.

**Corrosion and soiling effects by air pollution**

C. Tzanis et al.

Title Page

Abstract

Introduction

Conclusions

References

Tables

Figures

◀

▶

◀

▶

Back

Close

Full Screen / Esc

Printer-friendly Version

Interactive Discussion



(b) At a microscopic scale, particles from the soiled glass samples have been analysed and the average chemical composition of the deposited particles on the glass samples is presented in Fig. 13. In addition to the compounds presented in the figure, there were trace quantities of other soluble ions. CP stands for carbonaceous particles. It is remarkable that the main part of the deposited mass was insoluble.

Figure 14 shows the average chemical composition of the deposited mass on passive particle collectors, exposed at the same place as modern glass samples, during the same period (Tzanis et al., 2009). This chemical analysis did not include measurements for the carbonate content. The results for soluble ions composition are similar. The difference of the insoluble part of the deposited mass could be explained by the amount of carbonaceous particles.

### 3.4 Stone materials

For the evaluation of corrosion of the natural stone materials, recession, for the unsheltered specimens, and accumulation, for the sheltered ones, were calculated. These parameters were calculated by the formula  $\mu\text{m} = (W_1 - W_0)/(A\rho)$ , where  $W_0$  is weight before the exposure,  $W_1$  is weight after the exposure,  $A$  is the total surface area of sample and  $\rho$  is the density of the relevant stone.

For the concrete material the corrosion rate was expressed as mass changes in percentage. The results of recession for the specimens exposed, under unsheltered conditions, for one year are presented in Fig. 15 (Massey and Yates, 2004). According to these results Saaremaa dolomite was the most sensitive stone, among the exposed, to recession while Carrara marble the most durable. This result was expected for Carrara marble because of its physical properties. It presents high density, low porosity and water absorption, the ideal properties for a durable material. Saaremaa dolomite presents high water absorption, saturation coefficient and porosity suggesting low weatherability which is confirmed by these results.

The results of accumulation for the specimens exposed under sheltered conditions, also for one year, can be found in Fig. 16. Carrara marble presented the lowest value

of accumulation, close to zero, while Baumberger sandstone presented the highest, almost 6  $\mu\text{m}$ . Concrete samples, both sheltered and unsheltered, presented an increase of mass of about 2.5%. This observation could be explained by the active chemical reactions which take place between environment and concrete components and form hardly water soluble components. Rainwater cannot wash away these products, which accumulate on the sample, increasing its mass.

## 4 Summary

According to the above mentioned results, for the metal and alloy specimens exposed at specific height levels, the highest value of weight change for the unalloyed carbon steel was noticed at the level of 18 m, while the lowest was at the level of 6 m. For zinc and copper specimens, values of weight change were almost constant with the height and about 4 times lower than steel. Unalloyed carbon steel was shown to be the most sensitive material, among the exposed ones, also to the mass loss, while copper was the most durable. For all the samples, the lowest values of mass loss were noticed at the level of 6 m and increased with the height.

These parameters were also calculated for the specimens exposed on the main rack. Unalloyed carbon steel was the material with the greatest value of weight change, while bronze was the only material with negative value of this parameter. The mass loss of unalloyed carbon steel was more than 15 times greater than the other materials. Copper and bronze, with almost equal values of mass loss, suffered less by atmospheric corrosion. Zinc mass loss values were almost 70% greater than the same values of copper and bronze. The chemical analysis of the deposited mass on the above mentioned specimens revealed that sulphate dominated the other substances.

For all the exposed medieval glass specimens, an increase of the leaching depth was detected, mainly for K and Ca. The highest values of leaching depth, almost 50% higher than all other specimens, are noticed at medieval glass specimens exposed at the level of 21 m and on the roof. The rate of increase of the leaching depth for the

## Corrosion and soiling effects by air pollution

C. Tzanis et al.

Title Page

Abstract

Introduction

Conclusions

References

Tables

Figures

◀

▶

◀

▶

Back

Close

Full Screen / Esc

Printer-friendly Version

Interactive Discussion



specimens exposed on the main rack decreased with time, unlike the same rates of the specimens exposed at specific levels, which were increased with time.

The results for the modern glass samples indicate that the increasing trend of the total deposited mass of particles per surface unit and haze, demonstrates a cumulative non-linear phenomenon with an asymptotic level of saturation. In addition, the results of the chemical analysis of the deposited mass agree with a similar analysis, which was accomplished with passive particle collectors, exposed at the same place and for almost the same period.

For all natural stone materials, exposed under unsheltered conditions, surface recession was noticed. Saaremaa dolomite proves to be the most sensitive stone to weathering processes, while Carrara marble is the most resistant. Surface accumulation is noticed for all natural stone samples exposed under sheltered conditions. Baumberger sandstone has the highest values of accumulation, in contrast to Carrara marble, which has accumulation values close to zero.

*Acknowledgements.* We gratefully acknowledge the Ministry of Health and Social Solidarity, Rolf Snethlage, Manfred Schreiner, Michael Melcher, Markus Faller, Gundars Mezinskis, Tim Yates and all the participants in the MULTI-ASSESS, a research project supported by the European Commission under the Fifth Framework Programme Key Action City of Tomorrow and Cultural Heritage.

## References

- Alexandris, D., Varotsos, C., Kondratyev, K. Y., and Chronopoulos, G.: On the altitude dependence of solar effective UV, *Phys. Chem. Earth PT C*, 24, 515–517, 1999.
- Cape, J. N., Tang, Y. S., van Dijk, N., Love, L., Sutton, M. A., and Palmer, S. C. F.: Concentrations of ammonia and nitrogen dioxide at roadside verges, and their contribution to nitrogen deposition, *Environ. Pollut.*, 132, 469–478, 2004.
- Chattopadhyay, S. and Chattopadhyay, G.: Comparative study among different neural net learning algorithms applied to rainfall time series, *Meteorol. Appl.*, 15, 273–280, 2008.

## Corrosion and soiling effects by air pollution

C. Tzanis et al.

Title Page

Abstract

Introduction

Conclusions

References

Tables

Figures

◀

▶

◀

▶

Back

Close

Full Screen / Esc

Printer-friendly Version

Interactive Discussion



**Corrosion and soiling effects by air pollution**

C. Tzanis et al.

Title Page

Abstract

Introduction

Conclusions

References

Tables

Figures

◀

▶

◀

▶

Back

Close

Full Screen / Esc

Printer-friendly Version

Interactive Discussion



Ebel, A., Memmesheimer, M., and Jakobs, H. J.: Chemical perturbations in the planetary boundary layer and their relevance for chemistry transport modelling, *Bound-Lay. Meteorol.*, 125, 265–278, 2007.

Feretis, E., Theodorakopoulos, P., Varotsos, C., Efstathiou, M., Tzanis, C., Xirou, T., Alexandridou, N., and Aggelou, M.: On the plausible association between environmental conditions and human eye damage, *Environ. Sci. Pollut. R.*, 9, 163–165, 2002.

Ferm, M., De Santis, F., and Varotsos, C.: Nitric acid measurements in connection with corrosion studies, *Atmos. Environ.*, 39, 6664–6672, 2005.

Ferm, M., Watt, J., O'Hanlon, S., De Santis, F., and Varotsos, C.: Deposition measurement of particulate matter in connection with corrosion studies, *Anal. Bioanal. Chem.*, 384, 1320–1330, 2006.

Friess, U., Monks, P. S., Remedios, J. J., Rozanov, A., Sinreich, R., Wagner, T., and Platt, U.: MAX-DOAS O<sub>4</sub> measurements: A new technique to derive information on atmospheric aerosols: 2. Modeling studies, *J. Geophys. Res.*, 111, D14203, doi:10.1029/2005JD006618, 2006.

Heard, D. E., Read, K. A., Methven, J., Al-Haider, S., Bloss, W. J., Johnson, G. P., Pilling, M. J., Seakins, P. W., Smith, S. C., Sommariva, R., Stanton, J. C., Still, T. J., Ingham, T., Brooks, B., De Leeuw, G., Jackson, A. V., McQuaid, J. B., Morgan, R., Smith, M. H., Carpenter, L. J., Carslaw, N., Hamilton, J., Hopkins, J. R., Lee, J. D., Lewis, A. C., Purvis, R. M., Wevill, D. J., Brough, N., Green, T., Mills, G., Penkett, S. A., Plane, J. M. C., Saiz-Lopez, A., Worton, D., Monks, P. S., Fleming, Z., Rickard, A. R., Alfarra, M. R., Allan, J. D., Bower, K., Coe, H., Cubison, M., Flynn, M., McFiggans, G., Gallagher, M., Norton, E. G., O'Dowd, C. D., Shillito, J., Topping, D., Vaughan, G., Williams, P., Bitter, M., Ball, S. M., Jones, R. L., Povey, I. M., O'Doherty, S., Simmonds, P. G., Allen, A., Kinnersley, R. P., Beddows, D. C. S., Dall'Osto, M., Harrison, R. M., Donovan, R. J., Heal, M. R., Jennings, S. G., Noone, C., and Spain, G.: The North Atlantic Marine Boundary Layer Experiment (NAMBLEX). Overview of the campaign held at Mace Head, Ireland, in summer 2002, *Atmos. Chem. Phys.*, 6, 2241–2272, doi:10.5194/acp-6-2241-2006, 2006.

Horalek, S., Kuxenko, S., Singer, B., Wiedemann, G., and Woznik, E.: Model for multipollutant impact and assessment of threshold levels for cultural heritage, Evaluation of corrosion attack on copper and bronze of the broad field and targeted field exposure programme, EU 5FP RTD Project (project homepage: <http://www.corr-institute.se/MULTI-ASSESS/web/page.aspx>), 2005.

## Corrosion and soiling effects by air pollution

C. Tzanis et al.

Title Page

Abstract

Introduction

Conclusions

References

Tables

Figures

◀

▶

◀

▶

Back

Close

Full Screen / Esc

Printer-friendly Version

Interactive Discussion



Ionescu, A., Lefèvre, R.-A., Chabas, A., Lombardo, T., Ausset, P., Candau, Y., and Rosseman, L.: Modeling of soiling based on silica-soda-lime glass exposure at six European sites, *Sci. Total Environ.*, 369, 246–255, 2006.

Katsambas, A., Varotsos, C. A., Veziryianni, G., and Antoniou, C.: Surface solar ultraviolet radiation: A theoretical approach of the SUVR reaching the ground in Athens, Greece, *Environ. Sci. Pollut. R.*, 4, 69–73, 1997.

Kondratyev, K. Y. and Varotsos, C. A.: Global total ozone dynamics – Impact on surface solar ultraviolet radiation variability and ecosystems, *Environ. Sci. Pollut. R.*, 3, 205–209, 1996.

Kucera, V., Tidblad, J., Kreislova, K., Knotkova, D., Faller, M., Sneath, R., Yates, T., Henriksen, J., Schreiner, M., Ferm, M., Lefèvre, R.-A., and Kobus, J.: The UN/ECE ICP Materials multi-pollutants exposure on effects on materials including historic and cultural monuments, in Conference Abstracts of the 7th International Conference on Acid Deposition, Prague, Czech Republic, 12–17 June 2005, 698, 2005.

Lombardo, T., Ionescu, A., Lefèvre, R.-A., Chabas, A., Ausset, P., and Cachier, H.: Soiling of silica-soda-lime float glass in urban environment: measurements and modelling, *Atmos. Environ.*, 39, 989–997, 2005.

Lombardo, T., Ionescu, A., Chabas, A., Lefèvre, R.-A., Ausset, P., and Candau, Y.: Dose-response function for the soiling of silica-soda-lime glass due to dry deposition, *Sci. Total Environ.*, 408, 976–984, 2010.

Massey, S. W. and Yates, T.: Model for multipollutant impact and assessment of threshold levels for cultural heritage, Deliverable 4.0, Completion and evaluation of targeted field exposure, use of results for model validation and assessment of uncertainties, EU 5FP RTD Project (project homepage: <http://www.corr-institute.se/MULTI-ASSESS/web/page.aspx>), 2004.

Melcher, M., and Schreiner, M.: Model for multipollutant impact and assessment of threshold levels for cultural heritage, Results of the Exposure of Potash-Lime-Silica Glasses within Work Package 4 of the MULTI-ASSESS Project, Final Report, EU 5FP RTD Project (project homepage: <http://www.corr-institute.se/MULTI-ASSESS/web/page.aspx>), 2004.

Melcher, M. and Schreiner, M.: Leaching studies on naturally weathered potash-lime-silica glasses, *J. Non-Cryst. Solids*, 352, 368–379, 2006.

Methven, J., Arnold, S. R., Stohl, A., Evans, M. J., Avery, M., Law, K., Lewis, A. C., Monks, P. S., Parrish, D. D., Reeves, C. E., Schlager, H., Atlas, E., Blake, D. R., Coe, H., Crosier, J., Flocke, F. M., Holloway, J. S., Hopkins, J. R., McQuaid, J., Purvis, R., Rappengluck, B., Singh, H. B., Watson, N. M., Whalley, L. K., and Williams, P. I.: Establishing Lagrangian connections

**Corrosion and soiling effects by air pollution**

C. Tzanis et al.

[Title Page](#)[Abstract](#)[Introduction](#)[Conclusions](#)[References](#)[Tables](#)[Figures](#)[◀](#)[▶](#)[◀](#)[▶](#)[Back](#)[Close](#)[Full Screen / Esc](#)[Printer-friendly Version](#)[Interactive Discussion](#)

between observations within air masses crossing the Atlantic during the International Consortium for Atmospheric Research on Transport and Transformation experiment, *J. Geophys. Res.*, 111, D23S62, doi:10.1029/2006JD007540, 2006.

Monks, P. S., Salisbury, G., Holland, G., Penkett, S. A., and Ayers, G. P.: A seasonal comparison of ozone photochemistry in the remote marine boundary layer, *Atmos. Environ.*, 34, 2547–2561, 2000.

Ondov, J. M., Buckley, T. J., Hopke, P. K., Ogulei, D., Parlange, M. B., Rogge, W. F., Squibb, K. S., Johnston, M. V., and Wexler, A. S.: Baltimore Supersite: Highly time- and size-resolved concentrations of urban PM<sub>2.5</sub> and its constituents for resolution of sources and immune responses, *Atmos. Environ.*, 40, 224–237, 2006.

Singer, B., Doktor, A., and Woznik, E.: UN/ECE International Co-operative Programme on Effects on Materials, including Historic and Cultural Monuments, Report No 44: Results from the multipollutant programme: Corrosion attack on copper and bronze after 1, 2 and 4 years of exposure (1997–2001), Bavarian State Department of Historical Monuments, Munich, Germany, 2003.

Tidblad, J., Kucera, V., Mezinskas, G., and Sidraba, I.: Model for multipollutant impact and assessment of threshold levels for cultural heritage, Deliverable D4.1, Completion and evaluation of targeted stone exposure, EU 5FP RTD Project (project homepage: <http://www.corr-institute.se/MULTI-ASSESS/web/page.aspx>), 2005.

Tidblad, J., Kucera, V., and Mikhailov, A. A.: UN/ECE International Co-operative Programme on Effects on Materials, including Historic and Cultural Monuments, Report No 30: Statistical analysis of 8 year materials exposure and acceptable deterioration and pollution levels, Swedish Corrosion Institute, Stockholm, Sweden, 1998.

Tzanis, C. and Varotsos, C. A.: Tropospheric aerosol forcing of climate: a case study for the greater area of Greece, *Int. J. Remote Sens.*, 29, 2507–2517, 2008.

Tzanis, C., Varotsos, C., Ferm, M., Christodoulakis, J., Assimakopoulos, M. N., and Efthymiou, C.: Nitric acid and particulate matter measurements at Athens, Greece, in connection with corrosion studies, *Atmos. Chem. Phys.*, 9, 8309–8316, doi:10.5194/acp-9-8309-2009, 2009.

Varotsos, C. A., Chronopoulos, G. J., Katsikis, S., and Sakellariou, N. K.: Further evidence of the role of air-pollution on solar ultraviolet-radiation reaching the ground, *Int. J. Remote Sens.*, 16, 1883–1886, 1995.

Varotsos, C., Tzanis, C., and Cracknell, A.: The enhanced deterioration of the cultural heritage monuments due to air pollution, *Environ. Sci. Pollut. R.*, 16, 590–592, 2009.



**Fig. 1.** The exposure site in Athens, Greece. The top panel shows the aluminium racks mounted at the heights of 3, 6, 9, 15, 18 and 21 m (not visible from this side), on a building, located in the Athens centre. The middle panel shows the group of three aluminium racks (on the left) with the specimens (on the right) which were distributed on the east facade of the building. The bottom panel shows the wooden rack (main rack) which was installed on the roof and consisted of an inclined plane (on the left) and an aluminium box with open bottom (on the right).

**Corrosion and soiling effects by air pollution**

C. Tzanis et al.

Title Page

Abstract

Introduction

Conclusions

References

Tables

Figures

◀

▶

◀

▶

Back

Close

Full Screen / Esc

Printer-friendly Version

Interactive Discussion



**Corrosion and soiling effects by air pollution**

C. Tzanis et al.

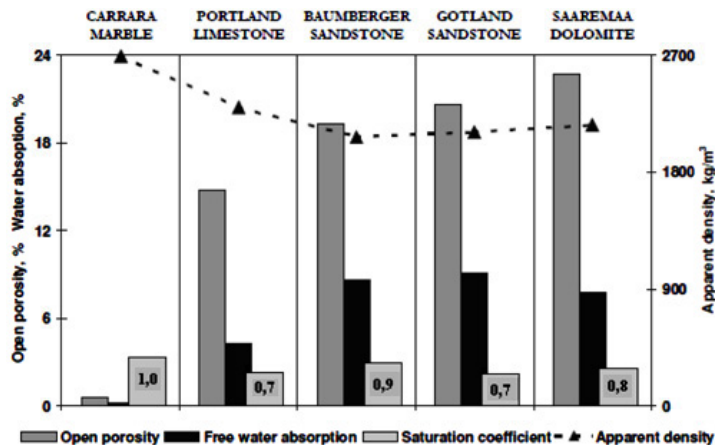


Fig. 2. Physical properties of stone materials.

Title Page

Abstract Introduction

Conclusions References

Tables Figures

◀ ▶

◀ ▶

Back Close

Full Screen / Esc

Printer-friendly Version

Interactive Discussion



**Corrosion and soiling effects by air pollution**

C. Tzanis et al.

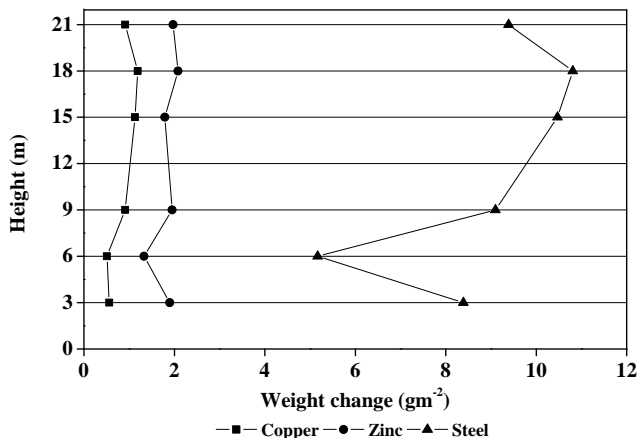


**Fig. 3.** Weight change of the specimens exposed for one year at specific levels (sheltered).

Title Page

Abstract Introduction

Conclusions References

Tables Figures

◀ ▶

◀ ▶

Back Close

Full Screen / Esc

Printer-friendly Version

Interactive Discussion



**Corrosion and soiling effects by air pollution**

C. Tzanis et al.

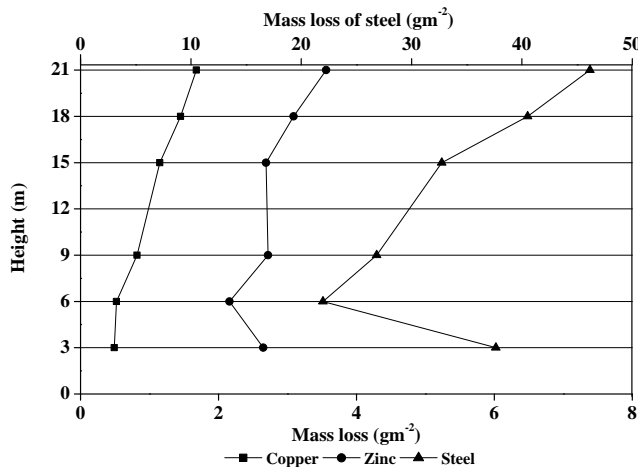


**Fig. 4.** Mass loss of the specimens exposed for one year at specific levels (sheltered).

Title Page

Abstract Introduction

Conclusions References

Tables Figures

◀ ▶

◀ ▶

Back Close

Full Screen / Esc

Printer-friendly Version

Interactive Discussion



**Corrosion and soiling effects by air pollution**

C. Tzanis et al.

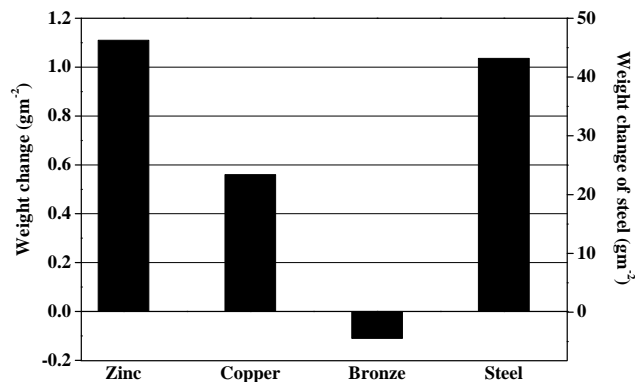


**Fig. 5.** Weight change of the specimens exposed for one year on the main rack (unsheltered).

Title Page

Abstract

Introduction

Conclusions

References

Tables

Figures

◀

▶

◀

▶

Back

Close

Full Screen / Esc

Printer-friendly Version

Interactive Discussion



**Corrosion and soiling effects by air pollution**

C. Tzanis et al.

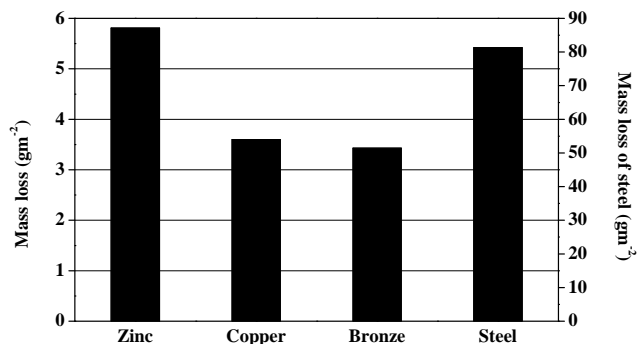


**Fig. 6.** Mass loss of the specimens exposed for one year on the main rack (unsheltered).

[Title Page](#)[Abstract](#)[Introduction](#)[Conclusions](#)[References](#)[Tables](#)[Figures](#)[⏪](#)[⏩](#)[◀](#)[▶](#)[Back](#)[Close](#)[Full Screen / Esc](#)[Printer-friendly Version](#)[Interactive Discussion](#)

## Corrosion and soiling effects by air pollution

C. Tzanis et al.

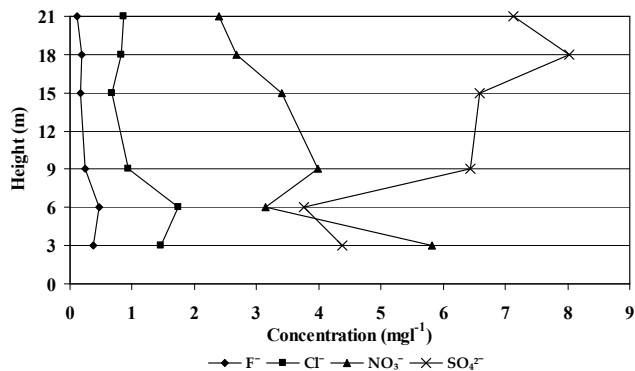


**Fig. 7.** Concentration of the water-soluble anions on the copper specimens exposed for one year as a function of height.

[Title Page](#)
[Abstract](#)
[Introduction](#)
[Conclusions](#)
[References](#)
[Tables](#)
[Figures](#)
[◀](#)
[▶](#)
[◀](#)
[▶](#)
[Back](#)
[Close](#)
[Full Screen / Esc](#)
[Printer-friendly Version](#)
[Interactive Discussion](#)


**Corrosion and soiling effects by air pollution**

C. Tzanis et al.

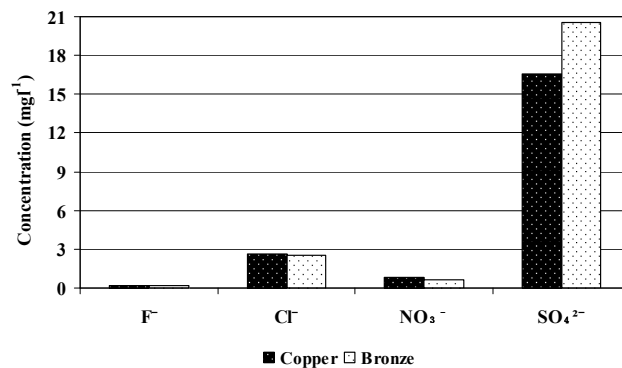


**Fig. 8.** Concentration of the water-soluble anions on the copper and bronze specimens exposed for one year on the main rack.

[Title Page](#)[Abstract](#)[Introduction](#)[Conclusions](#)[References](#)[Tables](#)[Figures](#)[◀](#)[▶](#)[◀](#)[▶](#)[Back](#)[Close](#)[Full Screen / Esc](#)[Printer-friendly Version](#)[Interactive Discussion](#)

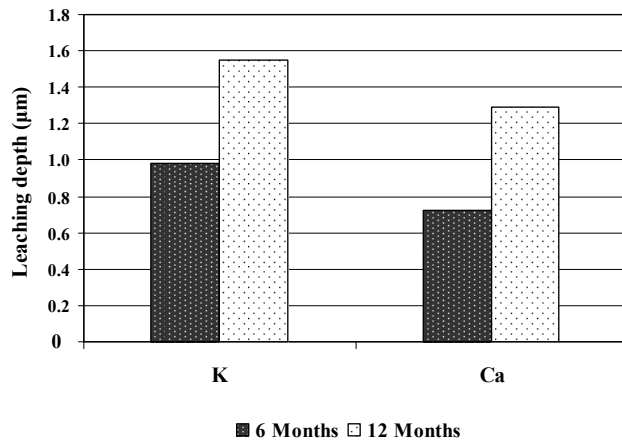


**Fig. 9.** Leaching depth of the specimens exposed on the main rack.

**Corrosion and soiling effects by air pollution**

C. Tzanis et al.

Title Page

Abstract Introduction

Conclusions References

Tables Figures

◀ ▶

◀ ▶

Back Close

Full Screen / Esc

Printer-friendly Version

Interactive Discussion



**Corrosion and soiling effects by air pollution**

C. Tzanis et al.

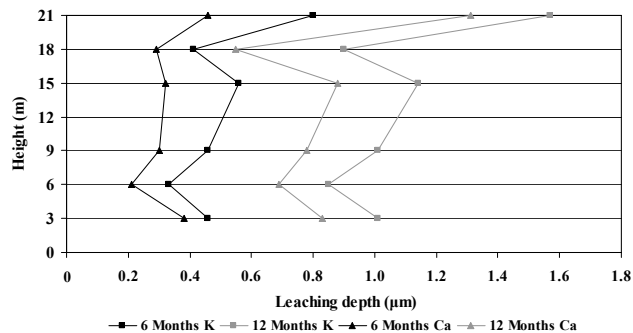


**Fig. 10.** Leaching depth of the specimens as a function of height.

Title Page

Abstract

Introduction

Conclusions

References

Tables

Figures

◀

▶

◀

▶

Back

Close

Full Screen / Esc

Printer-friendly Version

Interactive Discussion



**Corrosion and soiling effects by air pollution**

C. Tzanis et al.

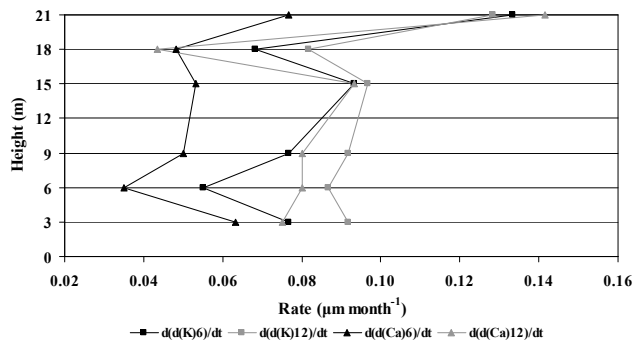


**Fig. 11.** Rate of increase of leaching depth for all specimens as a function of height.

Title Page

Abstract

Introduction

Conclusions

References

Tables

Figures

◀

▶

◀

▶

Back

Close

Full Screen / Esc

Printer-friendly Version

Interactive Discussion



**Corrosion and soiling effects by air pollution**

C. Tzanis et al.

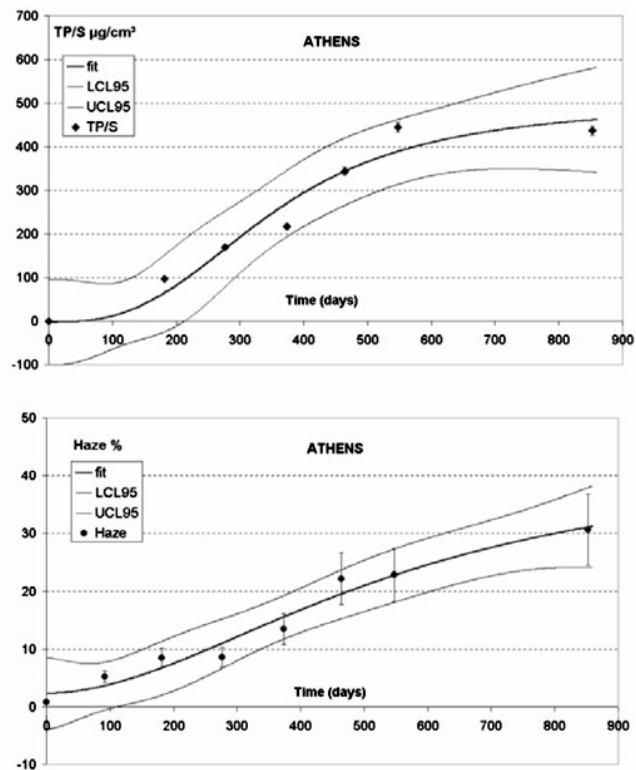


**Fig. 12.** Time evolution of TP/S ( $\mu\text{g cm}^{-2}$ ) and haze (%) for modern glass in Athens: best-fitting Hill model (fit) with the estimation confidence band (LCL95: Lower Confidence Level of 95%; UCL95: Upper Confidence Level of 95%) and experimental data with error bars (from Ionescu et al., 2006).

Title Page

Abstract

Introduction

Conclusions

References

Tables

Figures

◀

▶

◀

▶

Back

Close

Full Screen / Esc

Printer-friendly Version

Interactive Discussion



**Corrosion and soiling effects by air pollution**

C. Tzanis et al.

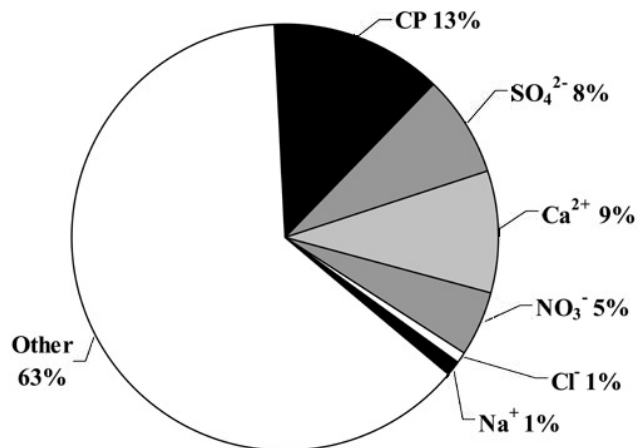


**Fig. 13.** Average chemical composition (mass percentage) of the deposited particles on the glass samples.

[Title Page](#)[Abstract](#)[Introduction](#)[Conclusions](#)[References](#)[Tables](#)[Figures](#)[◀](#)[▶](#)[◀](#)[▶](#)[Back](#)[Close](#)[Full Screen / Esc](#)[Printer-friendly Version](#)[Interactive Discussion](#)

**Corrosion and soiling effects by air pollution**

C. Tzanis et al.

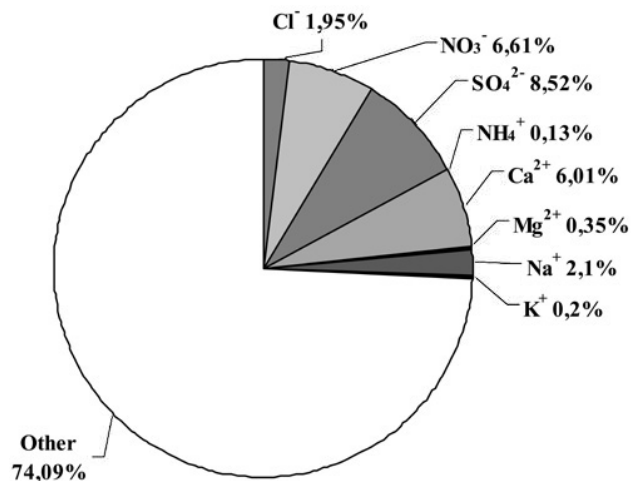


**Fig. 14.** Average chemical composition (mass percentage) of the deposited particles on passive particle collectors.

[Title Page](#)[Abstract](#)[Introduction](#)[Conclusions](#)[References](#)[Tables](#)[Figures](#)[◀](#)[▶](#)[◀](#)[▶](#)[Back](#)[Close](#)[Full Screen / Esc](#)[Printer-friendly Version](#)[Interactive Discussion](#)

**Corrosion and soiling effects by air pollution**

C. Tzanis et al.

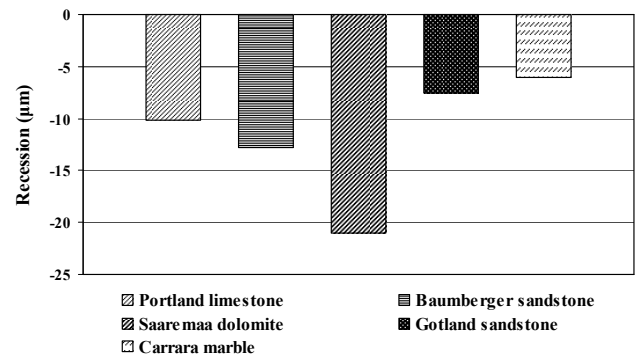


**Fig. 15.** Recession of natural stone materials exposed for one year under unsheltered conditions.

Title Page

Abstract

Introduction

Conclusions

References

Tables

Figures

◀

▶

◀

▶

Back

Close

Full Screen / Esc

Printer-friendly Version

Interactive Discussion



**Corrosion and soiling effects by air pollution**

C. Tzanis et al.

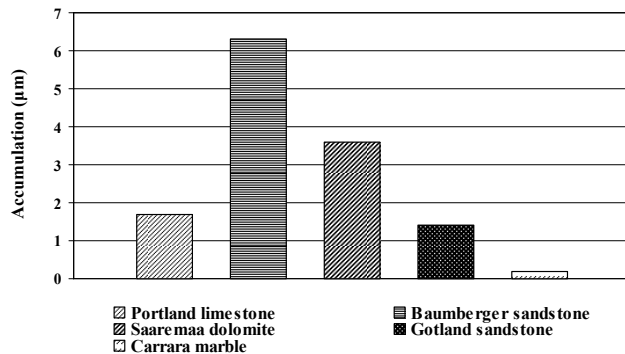


**Fig. 16.** Accumulation of natural stone materials exposed for one year under sheltered conditions.

Title Page

Abstract

Introduction

Conclusions

References

Tables

Figures

◀

▶

◀

▶

Back

Close

Full Screen / Esc

Printer-friendly Version

Interactive Discussion

